ACS OMEGA

http://pubs.acs.org/journal/acsodf

Article

Toward Point-of-Care Diagnostics to Monitor MMP-9 and TNF-α Levels in Inflammatory Bowel Disease

Dandan Liu, Emilie Viennois, Jieqiong Fang, Didier Merlin, and Suri S. Iyer*

Cite This: *ACS Omega* 2021, 6, 6582−6587

Read Online

ACCESS | Metrics & More | Article Recommendations | Supporting Information

ABSTRACT: We have investigated the association of matrix metallopeptidase 9 (MMP-9) and tumor necrosis factor α (TNF-α) levels with colitis severity using an established IL10−/− mouse model, which reflects the severity of inflammation in humans with inflammatory bowel disease (IBD). We found that MMP-9 and TNF-α correlated with colitis severity. In parallel, we developed assays to detect fecal MMP-9 and serum TNF-α using "cap and release" mesoporous silica nanoparticles (MSNs). MMP-9 peptide substrates as "caps" were attached to dye-loaded MSNs. The introduction of MMP-9 resulted in substrate cleavage and subsequent dye release, which was rapidly detected using a fluorometer. For TNF-α, an anti-TNF antibody was used as the "cap". The introduction of TNF-α antigen leads to the release of the dyes because the antigen binds more strongly to the antibody cap. The MSN-based assays can detect MMP-9 and TNF-α effectively, although signal amplification is required to meet clinical sensitivity.

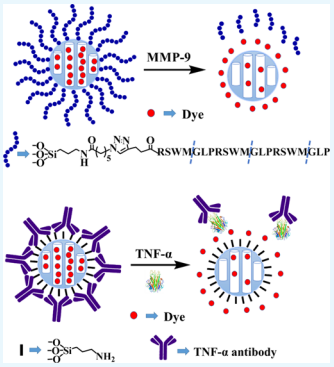

INTRODUCTION

Inflammatory bowel disease (IBD) is characterized by chronic inflammation of the gastrointestinal tract.[1] Ulcerative colitis (UC) and Crohn's disease (CD) are two major subtypes of IBD. Global cases of IBD have risen significantly from 3.7 million in 1990 to an estimated 6.8 million in 2017.[2] Patients with IBD require long-term management and frequent follow-ups with their physician. The gold standard to detect and manage IBD is an endoscopic evaluation to monitor inflammation, and the procedure may be combined with a biopsy to determine if there is a cancerous growth.[3] However, this method is invasive and patients often experience pain and discomfort during these procedures, highlighting the need for a noninvasive and cost-effective technique to monitor inflammation. The concentration of fecal calprotectin is correlated with both endoscopic and histological inflammation scores in IBD.[3] Although a noninvasive procedure, the current assay for fecal calprotectin is not user-friendly and perceived as expensive for point-of-care diagnosis. Here, we have explored the value of matrix metallopeptidase 9 (MMP-9) and tumor necrosis factor α (TNF-α) as alternative biomarkers. The level of MMP-9, a 92 kDa gelatinase, increases during inflammation in IBD patients and is released in urine, stool, and blood.[4,5] TNF-α also increases during inflammation in serum.[6] The main goal of this study is to explore the correlation between concentrations of MMP-9, TNF-α, and severity of colitis in the IL10−/− mouse model. Since the IL10−/− mouse model exhibits inflammation similar to that in human IBD patients, we expect similar levels of inflammation in humans with IBD. However, we note that this study uses an animal model and further studies are required to determine if the biomarker inflammation levels are elevated to the same degree in humans with IBD.

In recent years, mesoporous silica nanoparticles (MSNs) have been a considerable focus of research attention as a drug delivery system. Due to their unique propensities, such as large loading capacity,[7,8] homogeneous porosity, inertness, and easy functionalization, MSNs have been widely used in diagnostics,[9,10] drug delivery,[11−13] sensing,[14,15] and bioimaging.[16] The external surface can be easily modified and capped with small molecules[17,18] and biomolecules.[19] A variety of triggers, such as light,[16] pH,[14,17] small molecules,[19,20] and biomolecules,[21] facilitate the opening of the gate to release the cargo within the pore. Here, we used MSNs to rapidly detect MMP-9 and TNF-α. First, we developed an assay using an MMP-9 substrate to cap MSNs; when MMP-9 is introduced in a sample, the enzyme opens the cap via cleavage of the substrate and the contents, i.e., the dye is released. A second assay was also developed, where TNF-α antibody is used to cap MSN; when samples containing TNF-α antigen is introduced, the antigen binds strongly to the antibody to open the cap and release the dyes (see Figures 1 and 2).

Received: October 20, 2020
Accepted: December 22, 2020
Published: March 3, 2021

https://dx.doi.org/10.1021/acsomega.0c05115
ACS Omega 2021, 6, 6582−6587

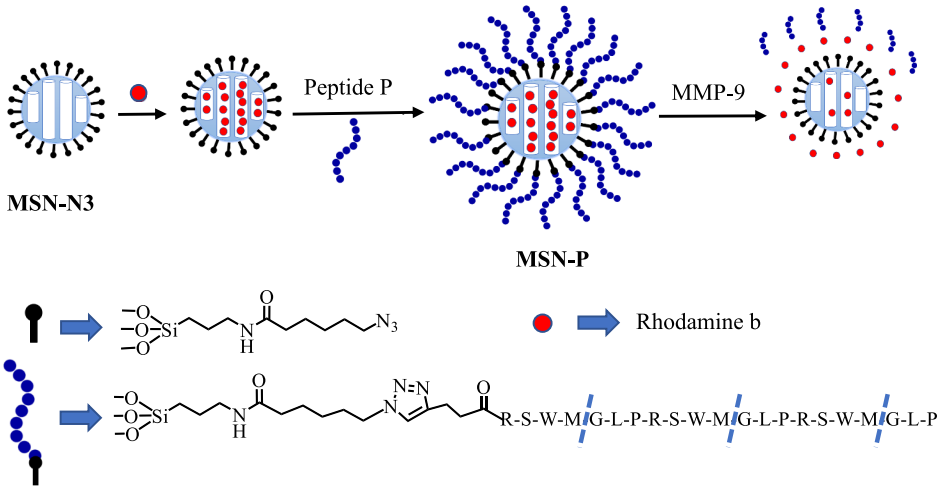

Figure 1. Experimental design of MMP-9 substrate capped MSN. The external surface of MSN was modified by the azide group. Rhodamine b was loaded and capped using the peptide substrate. The introduction of MMP-9 releases the dye by cleaving the substrate.

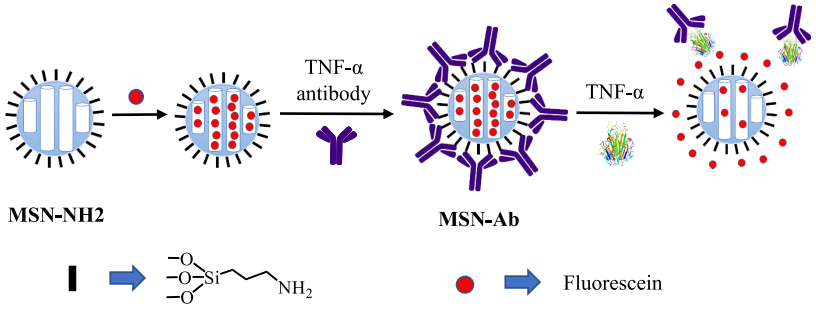

Figure 2. Experimental design of TNF-α antibody capped MSN. MSN was modified by (3-aminopropyl) triethoxysilane (APTES) to afford MSN-NH_2. After loading the dye, the negatively charged TNF-α antibody was used to cap the nanoparticles. Introduction of TNF-α antigen results in tight binding of the antibody to the antigen and opens the cap to release the dye.

RESULTS AND DISCUSSION

Association between MMP-9 and TNF-α Levels with IBD Severity. *MMP-9 Detection with IL10−/− Mouse Model.* First, we established the concentration of MMP-9 to monitor inflammation in wild-type and IL10−/− mice. The IL10−/− mouse model is a genetic model that spontaneously develops colitis with age.[22] The mice fecal samples of wild-type (mice without colitis) and IL10−/− (with colitis) groups were detected with InnoZyme Gelatinase (MMP-2/MMP-9) Activity Assay kit. The results showed that the MMP-9 level in the IL10−/− mice was significantly higher than that in the wild-type group (Figure 3A). The mean MMP-9 levels were 18 ± 3 ng/mL (n = 3) in wild-type mice and 31 ± 8 ng/mL (n = 3, $P < 0.05$) in IL10−/− mice. Next, we compared the MMP-9 levels among the IL10−/− mice of different ages, before (4 weeks old) and after mice developed colitis (14 weeks old) with the assay kit. The severity of the colitis increased with the ages of the IL10−/− mice.[22] The mean MMP-9 levels were 12 ± 20 ng/mL (n = 8) and 28 ± 22 ng/mL (n = 8, $P < 0.005$) in 4-week-old mice and 14-week-old mice, respectively, which shows that the MMP-9 levels were higher with increasing severity of colitis (Figure 3B). Fecal samples of the IL10−/− mice treated with anti-TNF-α antibody, which is commonly used to treat IBD,[23,24] and the nontreated IL10−/− mice that developed colitis were further compared (Figure 3C). The nontreated mice had higher levels (28 ± 22 ng/mL, n = 8) of MMP-9 than treated mice (7 ± 6 ng/mL, n = 8, $P < 0.05$), confirming that the MMP-9 concentration is correlated to the severity of colitis. Taken together, these studies confirm that the point-of-care diagnostics that monitor the MMP-9 levels could be used to monitor the inflammation associated with IBD.

TNF-α Detection with IL10−/− Mouse Model. We also established that the serum TNF-α content increases with the severity of IBD by comparing groups of mice of different ages, along with groups of anti-TNF-α-treated and nontreated IL10−/− mice (Figure 4). The differences in the TNF-α levels in mice serum from different age groups (week 4 and week 14) are presented in Figure 4A (mean TNF-α concentration in week 4 vs week 14 = 1.0 ± 0.9 vs 4.7 ± 2.6 pg/mL, n = 7 vs 7, $P < 0.01$). Our data clearly revealed the increasing TNF-α concentration in serum with the severity of colitis. Differences in the TNF-α levels in serum between anti-TNF-α-treated and nontreated mice are presented in Figure 4B (mean TNF-α concentration in nontreated vs treated = 4.7 ± 2.6 vs 1.3 ± 1.5 pg/mL, n = 7 vs 7, $P < 0.05$). The mean serum TNF-α content was significantly higher in nontreated than in treated mice in our experiments. Based on these findings, we propose that the colitis conditions may be effectively evaluated by monitoring the serum TNF-α concentration.

"Cap and Release" MSN to Detect MMP-9 and TNF-α. After establishing the limit and range of detection of the two biomarkers, MMP-9 and TNF-α in wild-type healthy and IL10−/− mice, we attempted to develop point-of-care diagnostics to monitor the inflammation associated with IBD.

https://dx.doi.org/10.1021/acsomega.0c05115
ACS Omega 2021, 6, 6582−6587

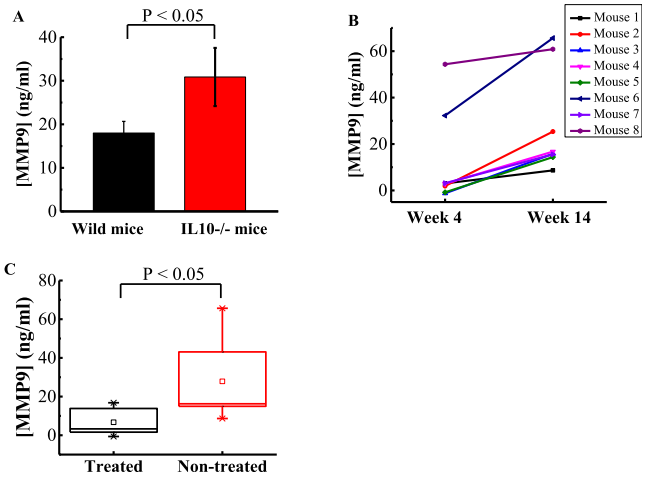

Figure 3. MMP-9 levels in wild-type and IL10−/− mice. (A) Difference in the fecal MMP-9 between wild mice (black column) and IL10−/− mice (red column) at 14 weeks old, detected by fluorescence. The mean concentration of fecal MMP-9 in IL10−/− mice (31 ± 8 ng/mL, n = 3) is significantly higher than that in wild mice (18 ± 3 ng/mL, n = 3, P < 0.05). (B) Difference in fecal MMP-9 in the IL10−/− mice of different ages. The mean concentration of fecal MMP-9 was detected by fluorescence at week 4 (12 ± 20 ng/mL, n = 8) and week 14 (28 ± 22 ng/mL, n = 8, P < 0.005). As age progresses, the concentration of fecal MMP-9 is higher. (C) Difference in fecal MMP-9 in anti-TNF-α-treated and nontreated IL10−/− mice. The mean concentration of fecal MMP-9 in nontreated mice (red box, 28 ± 22 ng/mL, n = 8) is higher than that in anti-TNF-α-treated mice (black box, 7 ± 6 ng/mL, n = 8, P < 0.05). All experiments were performed in triplicate, and the statistical method is pair-column t test from Origin.

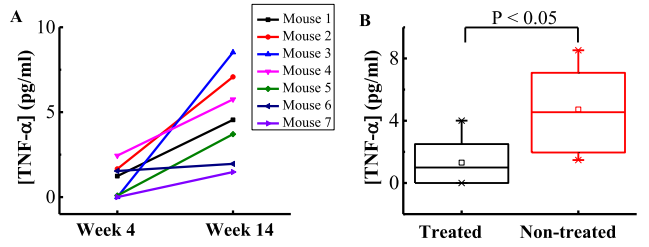

Figure 4. TNF-α level in the IL10−/− mice model. (A) Serum TNF-α concentration in IL10−/− mice of different ages. The mean concentration of serum TNF-α was detected by the purchased ELISA assay kit at week 4 (1.0 ± 0.9 pg/mL, n = 7) and week 14 (4.7 ± 2.6 pg/mL, n = 7, P < 0.01). As age progresses, the concentration of serum TNF-α is higher. (B) TNF-α levels between anti-TNF-α-treated and nontreated mice. The result shows that the concentration of serum TNF-α in nontreated mice (red box, 4.7 ± 2.6 pg/mL, n = 7) is significantly higher than that in treated mice (black box, 1.3 ± 1.5 pg/mL, n = 7, P < 0.05). All experiments were performed in triplicate, and the statistical method is pair-column t test from Origin.

MMP-9 Detection. We examined rhodamine b release for MMP-9 substrate capped MSN-P. Briefly, 1 mg of MSN-P was suspended in 1 mL of phosphate buffered saline (PBS) buffer and divided into two fractions, each containing 500 μg of MSN-P. One fraction was treated with 50 μL of PBS buffer as the control and another with 50 μL (0.1 mg/mL) of MMP-9. Both suspensions were incubated at 37 °C and the release of dye was detected at different time points. The results are shown in Figure 5A. Remarkable release of rhodamine b was observed in the presence of MMP-9 within minutes, while the release was minimal in its absence. This demonstrates that the

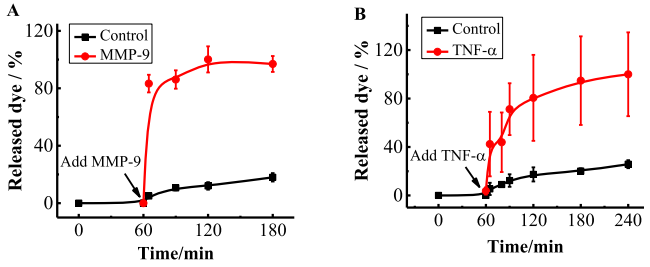

Figure 5. Detection of MMP-9 and TNF-α using dye-loaded MSNs. (A) In the presence (red line, filled circles) of fecal MMP-9, the dye release was significantly increased compared to that in the absence (black line, filled squares) of MMP-9. (B) Release study in the absence and presence of TNF-α. The released dye was significant in the presence (red line, filled circles) of TNF-α, while negligible release was found in the absence (black line, filled squares) of TNF-α. All experiments were performed in triplicate.

substrate cap was cleaved by MMP-9 to release the dye trapped in the pores of MSNs. To determine the limit of detection for MMP-9, we employed different concentrations for the release study (Figure S3). The limit of detection was measured as ~0.625 μg (1.1 μg/mL).

TNF-α Detection. We also examined the fluorescein release for TNF-α antibody capped MSNs, MSN-Ab. One milliliter of the suspended MSN-Ab in PBS was divided into two fractions, each containing 500 μL of MSN-Ab. One fraction was treated with 12 μL of PBS buffer as the control group and the other with 12 μL of 3 μg of TNF-α antigen as the experimental group. Fluorescein release from both groups was detected at different time points. The significant release was observed in the presence of TNF-α, while the release was relatively small in its absence (Figure 5B). Different concentrations of TNF-α were used for the release study to measure the limit of detection (Figure S4). The data showed that the limit of detection was around ~0.5 μg (1 μg/mL).

CONCLUSIONS

IBD is an inflammatory disease of the gastrointestinal tract. The IBD patients have to visit their physicians regularly to monitor inflammation, and the typical procedure is endoscopy, which causes significant distress and discomfort to the patient. Additionally, inflammatory flareups have been determined for a variety of reasons, including stress, environmental factors, etc., which make dosing of medication difficult for personalized medicine. If suitable biomarkers were identified in ex vivo body fluids, it would lead to an increase in research efforts to develop point-of-care diagnostics. Here, we investigated the association between fecal MMP-9 and serum TNF-α level due to inflammation using an established IL10−/− mouse model that has been used to determine the IBD severity.[22,25] We found that these two biomolecules could be potentially used to monitor inflammation in IBD. We note that these biomarkers are also elevated in other diseases like rheumatoid arthritis and, therefore, these biomarkers cannot be used to detect IBD. Rather, these biomarkers could potentially be used as biomarkers to manage inflammation in IBD patients, especially since inflammation flareups are unpredictable and can be caused by a number of triggers that include stress, change in environment, diet, etc. Once validated, these biomarkers could be developed further and incorporated in point-of-care diagnostics. The IBD patients could use these in the privacy of their homes and upload the results to their physicians

https://dx.doi.org/10.1021/acsomega.0c05115
ACS Omega 2021, 6, 6582−6587

electronically, who can adjust the dose of anti-inflammatory therapies for optimal management of the disease. We also developed assays to detect fecal MMP-9 and serum TNF-α. While the assays establish proof of concept that the dye-loaded MSNs can be used to monitor biomarker concentration and could be readily developed as the point-of-care diagnostics that require minimal sample pretreatment, the limit of detection is higher. Efforts to improve the sensitivity is currently underway, and these studies will be reported soon.

EXPERIMENTAL SECTION

Materials. InnoZyme Gelatinase (MMP-2/MMP-9) Activity Assay kit (CBA003) was purchased from Sigma-Aldrich. The fluorogenic substrate in the kit, (Gly-Pro-Hyp*)5-Gly-Pro-Lys(Mca)-Gly-Pro-Pro-Gly/Val-Val-Gly-Glu-Lys(Dnp)-Gly-Glu-Gln-(Gly-Pro-Hyp)5-NH2, is a FRET substrate; after cleavage, it releases fluorescence with an excitation/emission at 320/405 nm. Recombinant, active human MMP-9 (PF140), MCM-41-type mesostructured silica (CAS#: 7631-86-9), (3-aminopropyl) triethoxysilane (APTES, CAS#: 919-30-2) were purchased from Sigma. TNF α Mouse ELISA Kit, High Sensitivity (Catalog#: BMS607HS) was purchase from Thermo Fisher Scientific. Wild mice and IL10−/− mice serum and fecal samples were obtained from Didier Merlin (Georgia State University) lab.

MMP-9 and TNF-α Concentration Detection. *MMP-9 and TNF-α Activity Detection.* Fifty microliters of 1000 ng/mL MMP-9 enzyme was prepared, then 2-fold serial dilute 6 times with the PBS buffer in 96-well plate. Then, 50 μL of 30 μM MMP-9 substrate was added. The mixture was incubated at 37 °C for 3 h and then fluorescence was detected at 320/405 nm three times. The standard curve for the MMP-9 activity is shown in Figure S1A. TNF-α Mouse ELISA Kit, High Sensitivity was used for TNF-α activity detection and the manufacturer's instructions were followed for the experiment. The standard curve for the TNF-α activity is shown in Figure S1B.

Assays with Mice Fecal and Serum Samples. The mice feces were prepared as 100 mg/mL solution in the PBS buffer, vortexed for 15 min, centrifuged in 14 000*g* for 10 min and the supernatant was collected for the experiment. Next, 20 μL of the fecal sample was mixed with MMP-9 substrate to a total volume of 100 μL; the MMP-9 substrate final concentration was 15 μM. The mixture was incubated at 37 °C for 3 h and fluorescence was detected at 320/405 nm.

Fifty microliters of mice serum samples was used by TNF α Mouse ELISA Kit, High Sensitivity, Thermo Scientific, to detect TNF-α concentration in accordance with the manufacturer's instructions.

Fabrication and Characterization of MSNs. *Design and Synthesis of the MMP-9 Substrate-Gated Material.* We choose MCM-41, which is commercially available because this MSN is well characterized and has been used in several studies.[7,8,21] For the cap, we chose an MMP-9-specific substrate. MMP-9 specifically recognizes and cleaves the peptide sequence PLGMWSR. This peptide is specific to MMP-9 and not other proteases as demonstrated by Netzel-Arnett et al.[26,27] Accordingly, to fully cap the pore of MSN, a peptide, PLGMWSRPLGMWSRPLGMWSR-pentynoic acid (peptide P), containing three repeats of the MMP-9 substrate, PLGMWSR, and pentynoic acid at the end for pore capping was designed.[21] We choose three repeating units of the peptide to ensure minimal leakage of the dyes from the pores of MSN. In this system, the alkyne group of pentynoic acid reacts with the azide group modified on the surface of MSN and the cargo within the pore is released after peptide cleavage (Figure 1).

6-Azido-*N*-(3-(triethoxysilyl) propyl) hexanamide was synthesized according to Scheme S1. The compound was characterized completely by ^{1}H nuclear magnetic resonance (NMR) and ^{13}C NMR. Next, we modified MSN with 6-azido-*N*-(3-(triethoxysilyl) propyl) hexanamide. To this end, MCM-41 (0.1 g) was suspended in dry toluene (80 mL), followed by the addition of 6-azido-*N*-(3-(triethoxysilyl)propyl)-hexanamide (0.75 mL) and reflux for 24 h under a nitrogen atmosphere.[28] The mixture was centrifuged at 10 000 rpm for 10 min, washed with toluene and methanol, and dried under vacuum to obtain MSN-N3. To load the dye, a large excess of dye was used. Fifteen milligrams of MSN-N3 was suspended in 2.5 mL of 2 mg/mL rhodamine b solution in dimethylformamide (DMF) and stirred for 24 h. Next, 15 mg of peptide P, copper sulfate (11.24 mg) in 100 μL of DI water, sodium ascorbate (17.83 mg) in 100 μL of DI water, and 500 μL of *t*-butanol were added, and a microwave reaction was performed at 90 °C for 30 min.[29] The solution was centrifuged at 10 000 rpm for 5 min, washed with DI water, and dried under vacuum to generate MSN-P. This material was washed extensively 20 times with DI water, followed by PBS buffer over 10 days to remove the dye that was adhered on the surface.

Design and Synthesis of the TNF-α Antibody-Gated Material. First, the MSN surface was modified with (3-aminopropyl) triethoxysilane (APTES) to generate MSN-NH2, which was positively charged in the PBS buffer. MSN-NH2 was subsequently suspended in a fluorescein solution to load the dye via diffusion. Next, the negatively charged TNF-α antibody was added for the capping of MSN-NH2 via electrostatic interactions. The presented TNF-α antigen could bind the antibody, open the gate, and release the dye, which was detectable via fluorescence (Figure 2).

First, to modify the surface of MSN with APTES, the purchased MCM-41 (0.1 g) was suspended in dry toluene (80 mL) to which APTES (0.75 mL) was added, and refluxed for 24 h under a nitrogen atmosphere.[28] After the reaction, the mixture was centrifuged at 10 000 rpm for 10 min, washed with toluene and methanol, and dried under vacuum to generate MSN-NH2. The ζ-potential of MSN-NH2 was +14 mV, while that of MSN was −28 mV (Figure S2), confirming that the surface was covered by the amino group. Next, 10 mg of MSN-NH2 was suspended in 2 mL of 200 μM fluorescein PBS solution and stirred for 24 h, followed by the addition of 80 μL of 0.5 mg/mL TNF-α antibody and stirring for 6 h. The mixture was centrifuged at 10 000 rpm for 5 min, washed with PBS buffer, and dried to generate MSN-Ab. As described previously, this material was washed extensively to remove excess dye.

ASSOCIATED CONTENT

Supporting Information

The Supporting Information is available free of charge at https://pubs.acs.org/doi/10.1021/acsomega.0c05115.

Synthesis and graphics for the limit of detection (PDF)

https://dx.doi.org/10.1021/acsomega.0c05115
ACS Omega 2021, 6, 6582−6587

AUTHOR INFORMATION

Corresponding Author

Suri S. Iyer − *Department of Chemistry, Georgia State University, Atlanta, Georgia 30302, United States;* orcid.org/0000-0002-6196-006X; Email: siyer@gsu.edu

Authors

Dandan Liu − *Department of Chemistry, Georgia State University, Atlanta, Georgia 30302, United States*

Emilie Viennois − *Institute for Biomedical Sciences, Georgia State University, Atlanta, Georgia 30302, United States*

Jieqiong Fang − *Department of Chemistry, Georgia State University, Atlanta, Georgia 30302, United States*

Didier Merlin − *Institute for Biomedical Sciences, Georgia State University, Atlanta, Georgia 30302, United States; Atlanta Veterans Medical Center, Decatur, Georgia 30033, United States*

Complete contact information is available at: https://pubs.acs.org/10.1021/acsomega.0c05115

Notes

The authors declare no competing financial interest.

ACKNOWLEDGMENTS

The authors are grateful to the National Institute of Biomedical Imaging and Bioengineering (Grant Number R21-EB025049) for funding. D.M. is a recipient of a Senior Research Career Scientist Award (BX004476) from the Department of Veterans Affairs.

REFERENCES

(1) Hodson, R. Inflammatory bowel disease. *Nature* **2016**, *540*, No. S97.

(2) Alatab, S.; et al. The global, regional, and national burden of inflammatory bowel disease in 195 countries and territories, 1990-2017: a systematic analysis for the Global Burden of Disease Study 2017. *Lancet Gastroenterol. Hepatol.* **2020**, *5*, 17−30.

(3) D'Haens, G.; Ferrante, M.; Vermeire, S.; Baert, F.; Noman, M.; Moortgat, L.; Geens, P.; Iwens, D.; Aerden, I.; Van Assche, G.; Van Olmen, G.; Rutgeerts, P. Fecal calprotectin is a surrogate marker for endoscopic lesions in inflammatory bowel disease. *Inflammatory Bowel Dis.* **2012**, *18*, 2218−2224.

(4) Baugh, M. D.; Perry, M. J.; Hollander, A. P.; Davies, D. R.; Cross, S. S.; Lobo, A. J.; Taylor, C. J.; Evans, G. S. Matrix metalloproteinase levels are elevated in inflammatory bowel disease. *Gastroenterology* **1999**, *117*, 814−822.

(5) Farkas, K.; Sarodi, Z.; Balint, A.; Foldesi, I.; Tiszlavicz, L.; Szucs, M.; Nyari, T.; Tajti, J.; Nagy, F.; Szepes, Z.; Bor, R.; Annahazi, A.; Roka, R.; Molnar, T. The diagnostic value of a new fecal marker, matrix metalloprotease-9, in different types of inflammatory bowel diseases. *J. Crohn's Colitis* **2015**, *9*, 231−237.

(6) Komatsu, M.; Kobayashi, D.; Saito, K.; Furuya, D.; Yagihashi, A.; Araake, H.; Tsuji, N.; Sakamaki, S.; Niitsu, Y.; Watanabe, N. Tumor necrosis factor-alpha in serum of patients with inflammatory bowel disease as measured by a highly sensitive immuno-PCR. *Clin. Chem.* **2001**, *47*, 1297−1301.

(7) Climent, E.; Bernardos, A.; Martinez-Manez, R.; Maquieira, A.; Marcos, M. D.; Pastor-Navarro, N.; Puchades, R.; Sancenon, F.; Soto, J.; Amoros, P. Controlled Delivery Systems Using Antibody-Capped Mesoporous Nanocontainers. *J. Am. Chem. Soc.* **2009**, *131*, 14075−14080.

(8) de la Torre, C.; Mondragon, L.; Coll, C.; Sancenon, F.; Marcos, M. D.; Martinez-Manez, R.; Amoros, P.; Perez-Paya, E.; Orzaez, M. Cathepsin-B Induced Controlled Release from Peptide-Capped Mesoporous Silica Nanoparticles. *Chem. − Eur. J.* **2014**, *20*, 15309−15314.

(9) Rosenholm, J. M.; Sahlgren, C.; Linden, M. Multifunctional Mesoporous Silica Nanoparticles for Combined Therapeutic, Diagnostic and Targeted Action in Cancer Treatment. *Curr. Drug Targets* **2011**, *12*, 1166−1186.

(10) Oroval, M.; Climent, E.; Coll, C.; Eritja, R.; Avino, A.; Marcos, M. D.; Sancenon, F.; Martinez-Manez, R.; Amoros, P. An aptamer-gated silica mesoporous material for thrombin detection. *Chem. Commun.* **2013**, *49*, 5480−5482.

(11) Lu, C. H.; Willner, B.; Willner, I. DNA Nanotechnology: From Sensing and DNA Machines to Drug-Delivery Systems. *ACS Nano* **2013**, *7*, 8320−8332.

(12) Bitar, A.; Ahmad, N. M.; Fessi, H.; Elaissari, A. Silica-based nanoparticles for biomedical applications. *Drug Discovery Today* **2012**, *17*, 1147−1154.

(13) He, Q. J.; Shi, J. L. MSN Anti-Cancer Nanomedicines: Chemotherapy Enhancement, Overcoming of Drug Resistance, and Metastasis Inhibition. *Adv. Mater.* **2014**, *26*, 391−411.

(14) Wan, X. J.; Wang, D.; Liu, S. Y. Fluorescent pH-Sensing Organic/Inorganic Hybrid Mesoporous Silica Nanoparticles with Tunable Redox-Responsive Release Capability. *Langmuir* **2010**, *26*, 15574−15579.

(15) Tang, D.; Lin, Y.; Zhou, Q.; Lin, Y.; Li, P.; Niessner, R.; Knopp, D. Low-cost and highly sensitive immunosensing platform for aflatoxins using one-step competitive displacement reaction mode and portable glucometer-based detection. *Anal. Chem.* **2014**, *86*, 11451−11458.

(16) Zhang, X.; Yang, P. P.; Dai, Y. L.; Ma, P. A.; Li, X. J.; Cheng, Z. Y.; Hou, Z. Y.; Kang, X. J.; Li, C. X.; Lin, J. Multifunctional Up-Converting Nanocomposites with Smart Polymer Brushes Gated Mesopores for Cell Imaging and Thermo/pH Dual-Responsive Drug Controlled Release. *Adv. Funct. Mater.* **2013**, *23*, 4067−4078.

(17) Cauda, V.; Argyo, C.; Schlossbauer, A.; Bein, T. Controlling the delivery kinetics from colloidal mesoporous silica nanoparticles with pH-sensitive gates. *J. Mater. Chem.* **2010**, *20*, 4305−4311.

(18) Mas, N.; Galiana, I.; Hurtado, S.; Mondragon, L.; Bernardos, A.; Sancenon, F.; Marcos, M. D.; Amoros, P.; Abril-Utrillas, N.; Martinez-Manez, R.; Murguia, J. R. Enhanced antifungal efficacy of tebuconazole using gated pH-driven mesoporous nanoparticles. *Int. J. Nanomed.* **2014**, *9*, 2597−2605.

(19) Climent, E.; Martinez-Manez, R.; Maquieira, A.; Sancenon, F.; Marcos, M. D.; Brun, E. M.; Soto, J.; Amoros, P. Antibody-Capped Mesoporous Nanoscopic Materials: Design of a Probe for the Selective Chromo-Fluorogenic Detection of Finasteride. *ChemistryOpen* **2012**, *1*, 251−259.

(20) Luo, Z.; Hu, Y.; Cai, K. Y.; Ding, X. W.; Zhang, Q.; Li, M. H.; Ma, X.; Zhang, B. L.; Zeng, Y. F.; Li, P. Z.; Li, J. H.; Liu, J. J.; Zhao, Y. L. Intracellular redox-activated anticancer drug delivery by functionalized hollow mesoporous silica nanoreservoirs with tumor specificity. *Biomaterials* **2014**, *35*, 7951−7962.

(21) Coll, C.; Mondragon, L.; Martinez-Manez, R.; Sancenon, F.; Marcos, M. D.; Soto, J.; Amoros, P.; Perez-Paya, E. Enzyme-Mediated Controlled Release Systems by Anchoring Peptide Sequences on Mesoporous Silica Supports. *Angew. Chem., Int. Ed.* **2011**, *50*, 2138−2140.

(22) Keubler, L. M.; Buettner, M.; Hager, C.; Bleich, A. A Multihit Model: Colitis Lessons from the Interleukin-10-deficient Mouse. *Inflammatory Bowel Dis.* **2015**, *21*, 1967−1975.

(23) Adegbola, S. O.; Sahnan, K.; Warusavitarne, J.; Hart, A.; Tozer, P. Anti-TNF Therapy in Crohn's Disease. *Int. J. Mol. Sci.* **2018**, *19*, No. 2244.

(24) Zhang, C.; Shu, W.; Zhou, G.; Lin, J.; Chu, F.; Wu, H.; Liu, Z. Anti-TNF-alpha Therapy Suppresses Proinflammatory Activities of Mucosal Neutrophils in Inflammatory Bowel Disease. *Mediators Inflammation* **2018**, *2018*, No. 3021863.

(25) Wang, H.; Vilches-Moure, J. G.; Cherkaoui, S.; Tardy, I.; Alleaume, C.; Bettinger, T.; Lutz, A.; Paulmurugan, R. Chronic Model of Inflammatory Bowel Disease in IL-10(−/−) Transgenic Mice:

Evaluation with Ultrasound Molecular Imaging. *Theranostics* **2019**, *9*, 6031−6046.
(26) Tranchant, I.; Vera, L.; Czarny, B.; Amoura, M.; Cassar, E.; Beau, F.; Stura, E. A.; Dive, V. Halogen Bonding Controls Selectivity of FRET Substrate Probes for MMP-9. *Chem. Biol.* **2014**, *21*, 408−413.
(27) Netzel-Arnett, S.; Mallya, S. K.; Nagase, H.; Birkedal-Hansen, H.; Van Wart, H. E. Continuously recording fluorescent assays optimized for five human matrix metalloproteinases. *Anal. Biochem.* **1991**, *195*, 86−92.
(28) Tang, D. H.; Zhang, W. T.; Qiao, Z. N.; Liu, Y. L.; Huo, Q. S. Functionalized mesoporous silica nanoparticles as a catalyst to synthesize a luminescent polymer/silica nanocomposite. *RSC Adv.* **2016**, *6*, 16461−16466.
(29) Lee, J.; Kim, H.; Han, S.; Hong, E.; Lee, K. H.; Kim, C. Stimuli-Responsive Conformational Conversion of Peptide Gatekeepers for Controlled Release of Guests from Mesoporous Silica Nanocontainers. *J. Am. Chem. Soc.* **2014**, *136*, 12880−12883.

https://dx.doi.org/10.1021/acsomega.0c05115
ACS Omega 2021, 6, 6582−6587